JACS
JOURNAL OF THE AMERICAN CHEMICAL SOCIETY

COMMUNICATION

pubs.acs.org/JACS

Design of Chemical Shift-Switching ^{19}F Magnetic Resonance Imaging Probe for Specific Detection of Human Monoamine Oxidase A

Koya Yamaguchi,[†] Ryosuke Ueki,[†] Hiroshi Nonaka,[†] Fuminori Sugihara,[‡] Tetsuya Matsuda,[‡] and Shinsuke Sando*[,†,§]

[†]INAMORI Frontier Research Center, Kyushu University, 744 Motooka, Nishi-ku, Fukuoka 819-0395, Japan

[‡]Department of Systems Science, Graduate School of Informatics, Kyoto University, 36-1 Yoshida-Honmachi, Sakyo-ku, Kyoto 606-8501, Japan

[§]PRESTO, Japan Science and Technology Agency, 4-1-8 Honcho, Kawaguchi, Saitama 332-0012, Japan

Supporting Information

ABSTRACT: Monoamine oxidase (MAO) A is a flavoenzyme that catalyzes the oxidation of biologically important monoamines and is thought to be associated with psychiatric disorders. Here, we report a strategy for rationally designing a ^{19}F magnetic resonance imaging probe for the specific detection of human MAO-A (hMAO-A) activity. Our designed ^{19}F probe was oxidized expeditiously by hMAO-A to produce 2-fluoro-4-nitrophenol via a spontaneous β-elimination mechanism. Concomitant with the structural change of the probe to the product, the ^{19}F chemical shift changed by 4.2 ppm, which was enough to visualize the probe and enzymatic product separately. Importantly, our probe achieved excellent discrimination of hMAO-A from its isoform hMAO-B.

Monoamine oxidase (MAO) is a flavoenzyme that catalyzes the oxidation of monoamines to the corresponding iminium intermediates, which are subsequently hydrolyzed to aldehydes (Scheme 1).[1] In humans, MAO exists as two isoforms: hMAO-A and hMAO-B. These isoforms play different physiological roles.

hMAO-A oxidizes biologically important monoamine neurotransmitters, including serotonin and epinephrine, to maintain homeostasis. hMAO-A activity is thought to be associated with psychiatric disorders.[1] Current research suggests that brain hMAO-A increases in major depressive disorder (MDD), and elevated hMAO-A levels could be the primary cause of the monoamine-lowering process in MDD.[2] In fact, hMAO-A-selective inhibitors are prescribed as clinical antidepressant agents. By contrast, hMAO-B-selective inhibitors are devoid of such antidepressant activity.[2] In this sense, hMAO-A activity is one of the primary targets for psychiatric disorder analysis, and thus there is increasing focus on chemical probes that can selectively detect hMAO-A activity in a complex biological system.

To date, several optical hMAO indicators have been reported,[3−5] and some of these have realized the sensitive detection of hMAO activity in cells. However, these optical modality-based approaches typically suffer from difficulties when applied to ex vivo or in vivo applications because of the limited transparency of excitation and emission light through the opaque body.

In this context, magnetic resonance (MR) is an appropriate modality because MR signals can be detected even in deeper sites. In particular, a ^{19}F MR-based probe is most attractive because of the high sensitivity of ^{19}F (0.83 relative to ^{1}H) and extremely low background signals in biological samples.[6−9] ^{19}F-labeled compounds, such as fluorinated serotonin[7a] or dopamine,[7b] have potential for use in an ^{19}F-based MAO assay. To our knowledge, however, none of these has been shown to have MAO-A/B selectivity or to induce sufficient ^{19}F signal changes for ^{19}F magnetic resonance imaging (MRI). Under these circumstances, we were prompted to develop an hMAO-A-specific MRI probe. Here, we report a strategy for rationally designing a ^{19}F MRI probe targeting hMAO-A. Our probe achieved high specificity to hMAO-A and realized the ^{19}F chemical shift-based imaging of hMAO-A activity.

Scheme 1. Mechanism of Oxidative Deamination by MAO

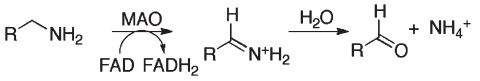

When designing an hMAO-A-specific ^{19}F MRI probe, there are two important issues to be solved. The first issue is how to incorporate hMAO-A specificity into the probe. hMAO-A and -B have about 70% identity,[1] and discriminating between these two isoforms is a challenge. We focused on hMAO inhibitors. Because hMAO inhibitors are used as potent pharmaceutical agents to treat psychiatric or neurodegenerative disorders, selective inhibitors have been investigated vigorously.[1b] Clorgyline (Figure 1a, left) is a known hMAO-A-selective inhibitor.[1a] Interestingly, structurally related pargyline (Figure 1a, second from left) is an inhibitor but is specific to hMAO-B.[1a] On the basis of this comparison, we hypothesized that *ortho*/*para*-substituted phenol (Figure 1a, third from left) is a key scaffold to achieve hMAO-A-selective binding.

The second issue is how to convert the *o*/*p*-substituted phenol, a hypothesized hMAO-A-selective binder, to the ^{19}F MRI probe. For this purpose, we designed compounds **1**−**3** as potent ^{19}F MRI probes with hMAO-A specificity (Figure 1a, right). These probes are designed to work as a ^{19}F chemical shift-switching probe via the following mechanism (see Figure 1b). After enzymatic oxidation of an amino group to aldehyde by MAO, a propionaldehyde moiety is released spontaneously by β-elimination in water to afford *o*/*p*-^{19}F/NO_2-phenol. Because of the electron-withdrawing property of the NO_2 substituent, the

Received: June 21, 2011
Published: August 18, 2011

dx.doi.org/10.1021/ja2057506 | *J. Am. Chem. Soc.* 2011, 133, 14208–14211

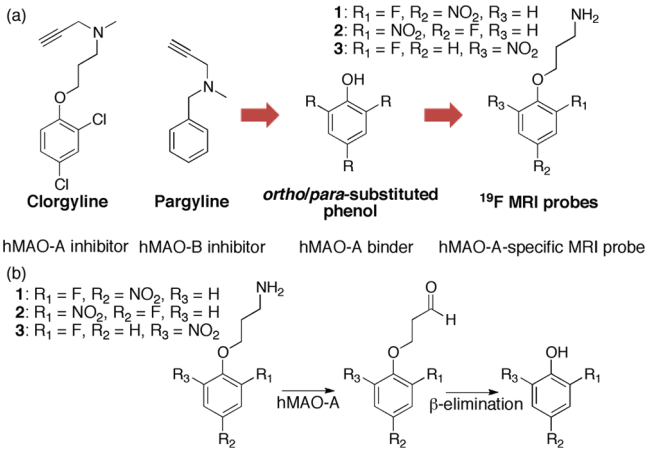

Figure 1. (a) Design of hMAO-A-specific ^{19}F MRI probes **1**−**3**. (b) Proposed mechanism for the spontaneous production of *o*/*p*-substituted phenol from ^{19}F MRI probes **1**−**3** upon oxidation by hMAO-A.

pK_a of the produced fluoronitrophenol is <7 (e.g., pK_a = 6.03 for 2-fluoro-4-nitrophenol[9c]), and the product should be present mainly as the phenolate form under physiological conditions. Thus, the net conversion from probes **1**−**3** to the *o*/*p*-^{19}F/NO$_2$-substituted phenolate ion should induce a sufficient chemical shift change of ^{19}F on the phenyl ring, as suggested by reports from Mason's group of a ^{19}F MRI reporter protein using an *o*/*p*-^{19}F/NO$_2$-phenol-based substrate.[9]

We first evaluated the reactivity of probes **1**−**3** to hMAO-A. Typically, the enzymatic reaction of probe (100 μM) by hMAO (12 units/mL) was performed in HEPES buffer (100 mM, pH 7.4) at 37 °C. After incubation with hMAO-A, intact probes were quantified by HPLC-UV analysis. During 1 h incubation, 65.8 ± 0.7, 10.5 ± 0.9, and 46.9 ± 1.1% of probes **1**, **2**, and **3** were consumed, respectively, suggesting that all three probes can be a substrate of hMAO-A and probe **1**, having a nitro substituent at the *para* position, is the best substrate among these probes (Figure 2a). This *p*-NO$_2$ selectivity is reasonable, based on crystallographic data of the clorgyline−hMAO-A complex, which shows a relatively wide space to accommodate the larger nitro group at the *para* position (Figure 2b).[10]

We focused further on the enzymatic reactivity of probe **1**. HPLC-UV analyses were performed at the λ_{max} of probe **1** (312 nm) and λ_{max} of the expected product 2-fluoro-4-nitrophenol (400 nm) (Figure 2c). After 1 h incubation with hMAO-A, the HPLC peak of probe **1** (15.8 min) was clearly reduced (top left vs top right at 312 nm). Monitoring at the λ_{max} of the enzymatic product (400 nm) showed concomitant appearance of a new peak at 10.6 min (Figure 2c, top right). The new peak was confirmed as the predicted 2-fluoro-4-nitrophenol by comparison with an authentic sample. Calculated from the peak intensity, the molar amount of 2-fluoro-4-nitrophenol produced corresponded to 66.0 ± 0.3% of probe **1**, indicating that about 100% of the consumed starting probe **1** was oxidized and converted expeditiously to 2-fluoro-4-nitrophenol via spontaneous β-elimination. These results validate the designed hMAO-A-induced deamination and β-elimination mechanism.

Very importantly, probe **1** showed high specificity for hMAO-A over hMAO-B. In contrast to the clear conversion by hMAO-A, only a faint amount (<1%) of the product was observed after incubation with hMAO-B (Figure 2c, bottom left). When the reaction with hMAO-A was performed in the presence of the

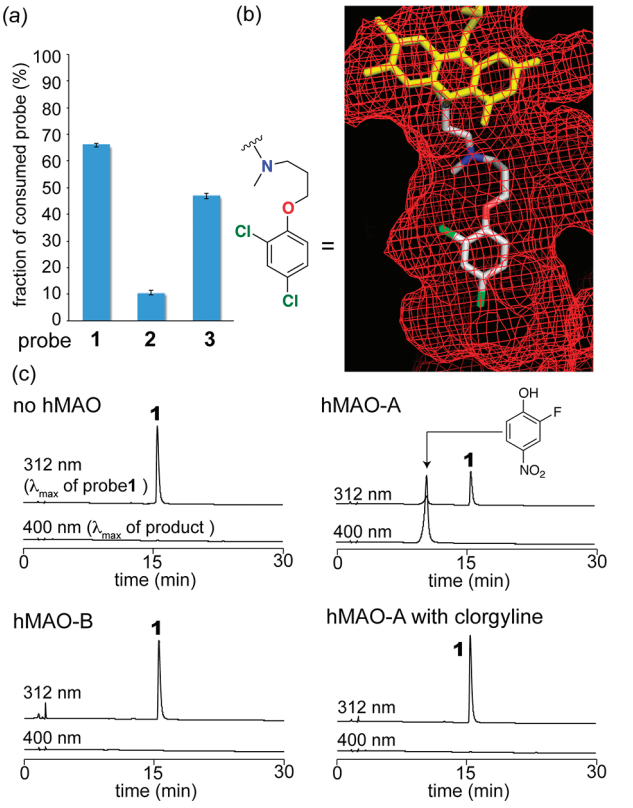

Figure 2. (a) Reactivity of probes **1**−**3** (100 μM) with hMAO-A (12 units/mL) in HEPES buffer (100 mM, pH 7.4) at 37 °C. The fraction of consumed probe was determined by HPLC-UV analysis of each enzymatic reaction solution. Error bars indicate the standard deviation of three independent experiments. (b) Active pocket of hMAO-A complexed with the inhibitor clorgyline and cofactor flavin adenine dinucleotide (FAD) (PDB: 2BXR). The chemical structure of clorgyline is shown to the left. The O, N, and Cl of clorgyline are depicted in red, blue, and green, respectively; FAD is shown in yellow. (c) HPLC-UV analyses (312 and 400 nm) of probe **1** (100 μM) after 1 h incubation: (top left) without hMAO-A, (top right) with hMAO-A (12 units/mL), (bottom left) with hMAO-B (12 units/mL), and (bottom right) with MAO-A (12 units/mL) and clorgyline (10 μM).

MAO-A inhibitor clorgyline (10 μM), production of 2-fluoro-4-nitrophenol was suppressed completely (Figure 2c, bottom right). The designed probe **1** worked as a substrate of hMAO-A with excellent specificity.

The enzymatic production of 2-fluoro-4-nitrophenol from probe **1** was also monitored by measuring the absorption. Upon reaction with hMAO-A (12 units/mL), the absorption spectra of probe **1** (100 μM) changed in an incubation time-dependent manner with a single isosbestic point at 345 nm (Figure 3a). The product 2-fluoro-4-nitrophenol (pK_a = 6.03[9c]) presented mainly in the phenolate ion form at physiological pH, so the product had an absorption maximum at a relatively long wavelength of 400 nm ($\varepsilon_{400\ nm}$ = 17 200 M^{-1} cm^{-1} in HEPES (100 mM, pH 7.4)). By contrast, the *o*-alkylated starting probe **1** had a low extinction coefficient at 400 nm. Therefore, the enzymatic conversion of **1** to product could be monitored easily by the absorption change at 400 nm. As shown in Figure 3b, a clear increase in absorption was observed for the probe **1** solution in the presence of hMAO-A (red circles). The presence of hMAO-B (green circles) or hMAO-A with the inhibitor clorgyline (blue circles) caused almost no absorption change. This specific

dx.doi.org/10.1021/ja2057506 |J. Am. Chem. Soc. 2011, 133, 14208–14211

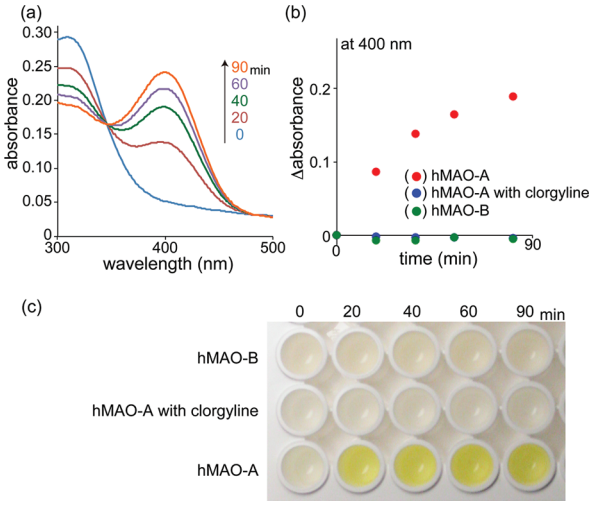

Figure 3. (a) Absorption spectra of probe **1** (100 μM) incubated with hMAO-A (12 units/mL) in HEPES buffer (pH 7.4) at 37 °C for 0, 20, 40, 60, and 90 min (from bottom to top at 400 nm). (b) Time course of the absorption change at 400 nm of probe **1** (100 μM) solution in the presence of hMAO-A (12 units/mL) (red), hMAO-A with the inhibitor clorgyline (10 μM) (blue), or hMAO-B (green). (c) Image of probe **1** solution (500 μM) incubated in the presence of hMAO-A (60 units/mL), hMAO-A with the inhibitor clorgyline (50 μM), and hMAO-B (from bottom to top) for 0, 20, 40, 60, and 90 min (from left to right).

reactivity of probe **1** to hMAO-A is consistent with the results obtained by HPLC-UV analysis (Figure 2).

Using the Michaelis−Menten equation, the kinetic parameters for enzymatic reaction of hMAO-A with probe **1** were determined as $K_m = 37.2 \pm 1.7$ μM and $V_{max} = 24.1 \pm 0.8$ nmol min^{-1} mg of microsomal protein^{-1}. The obtained K_m value is lower than that of natural monoamine substrates (high μM−mM range, e.g., $K_m = 137$ μM for serotonin[1b]), showing that probe **1** can be a practical substrate for hMAO-A under physiological conditions. By contrast, the reactivity of probe **1** with hMAO-B was too small to determine these parameters.

Because of the appreciable absorption enhancement at 400 nm, hMAO-A activity could be detected easily by the unaided eye. Figure 3c shows a photograph of probe **1** solutions in the presence of hMAO-A (bottom line), hMAO-A with clorgyline (middle line), and hMAO-B (top line). In the presence of hMAO-A, probe **1** solution turned yellow in an incubation time-dependent manner (from 0 to 90 min, from left to right). In marked contrast, the other solutions remained colorless. This indicates that probe **1** can also be used as a chromogenic probe for the specific sensing of hMAO-A activity. Although such chromogenic sensing is not our present concern, we note that this probe allows a mix-and-read sensing without the need for additional reagents, enzymes, or steps for monitoring. The hMAO-A/B selectivity, reactivity, and simplicity are superior to those reported for other chromogenic probes.[5]

Having an hMAO-A-specific substrate in hand, we moved on to the detection of hMAO-A activity using the ^{19}F MR modality. ^{19}F NMR analyses of probe **1** and product 2-fluoro-4-nitrophenol gave ^{19}F signals at −133.3 and −137.5 ppm, respectively (Figure 4a). The observed chemical shift difference between the probe and product was 4.2 ppm, which was enough to visualize each compound selectively using ^{19}F MRI. Figure 4b presents the phantom images (11.7 T) of these compounds in tubes. ^{1}H MRI

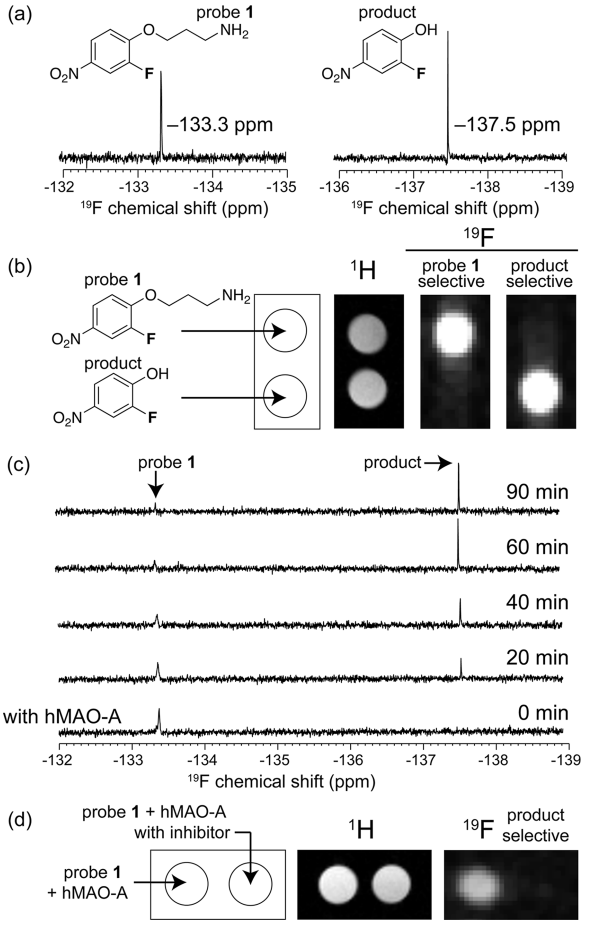

Figure 4. (a) ^{19}F NMR spectra of probe **1** and 2-fluoro-4-nitrophenol (100 μM) in HEPES buffer (pH 7.4). (b) ^{1}H and ^{19}F chemical shift-selective imaging (11.7 T) of probe **1** and 2-fluoro-4-nitrophenol (5 mM each) in HEPES buffer (pH 7.4). (c) Time course (0−90 min) of ^{19}F NMR spectra of probe **1** (100 μM) upon reaction with hMAO-A (12 units/mL). (d) ^{1}H and ^{19}F chemical shift-selective imaging (11.7 T) of hMAO-A activity (240 units/mL) using probe **1** (5 mM) in the presence or absence of the inhibitor clorgyline (250 μM).

visualized both tubes because of the presence of a large amount of H_2O (Figure 4b, left). By contrast, probe **1** and product 2-fluoro-4-nitrophenol were visualized separately by ^{19}F chemical shift-selective imaging (Figure 4b, middle and right, obtained by probe **1** and 2-fluoro-4-nitrophenol selective pulse frequencies, respectively).[11]

Finally, we applied probe **1** in ^{19}F MR analysis of hMAO activity. Probe **1** was incubated with hMAO-A, and the mixture was subjected to ^{19}F NMR analysis at each time point (0−90 min). At the starting point (0 min), a single ^{19}F peak was observed at −133.3 ppm (Figure 4c, bottom). As the reaction proceeded, a new signal appeared at −137.5 ppm in an incubation time-dependent manner (Figure 4c, from bottom to top, 0−90 min), which was assigned as the produced 2-fluoro-4-nitrophenol by comparison with an authentic sample. The time-course profile of ^{19}F NMR (79% conversion of probe **1** to product after the 90 min reaction, determined by comparison of the ^{19}F peak integrals) was similar to that observed by absorption analysis (Figure 3b) or HPLC-UV analysis (Figure S1, 78% conversion after 90 min, determined by HPLC), supporting that the ^{19}F NMR-based approach produces quantitative results. Again importantly, the new ^{19}F NMR peak at −137.5 ppm was

hMAO-A dependent. No signal was observed around −137.5 ppm after 60 min incubation with hMAO-B or hMAO-A in the presence of clorgyline (Figure S2). In addition to the hMAO-A specificity, it should be also noticed that a new NMR peak appeared in a clear probe-to-product one-to-one conversion manner without any undesirable side peaks. This is a big benefit for chemical shift-selective imaging, where sometimes such side peaks result in nonnegligible background or false-positive contrast. The designed probe **1** realized the direct imaging of hMAO-A activity (Figure 4d). ^{19}F chemical shift-selective imaging (product ^{19}F selective) produced the clear signal for probe **1** only upon incubation with hMAO-A (Figure 4d, left). The presence of an hMAO-A inhibitor completely suppressed such signal (Figure 4d, right). These results show clearly that the designed probe **1** functions as the first signal-switching ^{19}F MRI probe for the specific detection and imaging of hMAO-A activity.

In conclusion, we report a strategy for designing hMAO-A-specific ^{19}F MRI probe. The designed MRI probe has at least two distinct advantages. The first is specificity. On the basis of the *o*/*p*-substituted phenol hypothesis, our MRI probe achieved excellent discrimination of hMAO-A from its isoform hMAO-B. hMAO-A and -B play different physiological roles. In particular, hMAO-A, the focus of the present work, is considered one possible enzyme involved in the pathogenesis of psychiatric disorders.[2] In this sense, the specificity shown in this work is essential for revealing the true physiological and pathological roles of hMAO-A activity. The second advantage is the applicability to ^{19}F MRI. The rationally designed MRI probe achieved sufficient ^{19}F chemical shift change upon selective reaction with hMAO-A. These results allow us to conclude that the designed "smart" molecule functions as the first chemical shift-switching ^{19}F MRI probe for the specific detection and imaging of hMAO-A activity. In addition to the high performance of the present probe itself, the design strategy in this report may provide the basis for creating new hMAO-A- or -B-specific MRI probes.

Judging from the observation that the related ^{19}F-substituted phenol-type probes could be used successfully for in vivo ^{19}F NMR analysis of the reporter protein activity (e.g., 0.012−0.026 mmol of probes in the mouse experiments),[9] the present probe seems to have potential for in vivo applications. However, practical applications must await further experiments to improve the probe in terms of the enzymatic turnover rates and pharmacokinetic profiles. ^{19}F MR spectroscopy in a much larger voxel might also be a promising approach to overcome the intrinsic low sensitivity of the MR probe. In the future, the combination with PET studies should provide a more precise understanding of MAO activity.[12] Further work is in progress along these lines.

■ ASSOCIATED CONTENT

Supporting Information. Methods and Figures S1 and S2. This material is available free of charge via the Internet at http://pubs.acs.org.

■ AUTHOR INFORMATION

Corresponding Author
ssando@ifrc.kyushu-u.ac.jp

■ ACKNOWLEDGMENT

We thank Prof. Masahiro Shirakawa of Kyoto University for support on NMR measurements. This work was supported by NEXT Program and Grant-in-Aid No. 22685018 from JSPS, Japan, and partly by the Innovative Techno-Hub for Integrated Medical Bio-Imaging Project of the Special Coordination Funds for Promoting Science and Technology from MEXT, Japan.

■ REFERENCES

(1) For reviews on monoamine oxidase, see, for example: (a) Berry, M. D.; Juorio, A. V.; Paterson, I. A. *Prog. Neurobiol.* **1994**, *42*, 375–391. (b) Youdim, M. B.; Edmondson, D.; Tipton, K. F. *Nat. Rev. Neurosci.* **2006**, *7*, 295–309. (c) Edmondson, D. E.; Binda, C.; Wang, J.; Upadhyay, A. K.; Mattevi, A. *Biochemistry* **2009**, *48*, 4220–4230.

(2) (a) Meyer, J. H.; Boovariwala, A.; Sagrati, S.; Hussey, D.; Garcia, A.; Young, T; Praschak-Rieder, N.; Wilson, A. A.; Houle, S. *Arch. Gen. Psychiatry* **2006**, *63*, 1209–1216. (b) Robinson, D. S. *Primary Psychiatry* **2007**, *14*, 32–34.

(3) (a) Krajl, M. *Biochem. Pharmacol.* **1965**, *14*, 1684–1686. (b) Zhou, J. J. P.; Zhong, B.; Silverman, R. B. *Anal. Biochem.* **1996**, *234*, 9–12. (c) Zhou, M.; Panchuk-Voloshina, N. *Anal. Biochem.* **1997**, *253*, 169–174. (d) Chen, G.; Yee, D. J.; Gubernator, N. G.; Sames, D. *J. Am. Chem. Soc.* **2005**, *127*, 4544–4545. (e) Albers, A. E.; Rawls, K. A.; Chang, C. J. *Chem. Commun.* **2007**, 4647–4649. (f) Aw, J.; Shao, Q.; Yang, Y.; Jiang, T.; Ang, C.; Xing, B. *Chem. Asian J.* **2010**, *5*, 1317–1321.

(4) Zhou, W.; Valley, M. P.; Shultz, J.; Hawkins, E. M.; Bernad, L.; Good, T.; Good, D.; Riss, T. L.; Klaubert, D. H.; Wood, K. V. *J. Am. Chem. Soc.* **2006**, *128*, 3122–3123.

(5) (a) Tabor, C. W.; Tabor, H.; Rosenthal, S. M. *J. Biol. Chem.* **1954**, *208*, 645–661. (b) Weissbach, H.; Smith, T. E.; Daly, J. W.; Witkop, B.; Udenfriend, S. *J. Biol. Chem.* **1960**, *235*, 1160–1163. (c) Houslay, M. D.; Tipton, K. F. *Biochem. J.* **1974**, *139*, 645–652. (d) Flaherty, P.; Castagnoli, K.; Wang, Y.-X.; Castagnoli, N., Jr. *J. Med. Chem.* **1996**, *39*, 4756–4761. (e) Bissel, P.; Bigley, M. C.; Castagnoli, K.; Castagnoli, N., Jr. *Bioorg. Med. Chem.* **2002**, *10*, 3031–3041.

(6) (a) Cobb, S. L.; Murphy, C. D. *J. Fluorine Chem.* **2009**, *130*, 132–143. (b) Yu, J.-X.; Kodibagkar, V. D.; Cui, W.; Mason, R. P. *Curr. Med. Chem.* **2005**, *12*, 819–848.

(7) (a) Costa, J. L.; Dobson, C. M.; Fay, D. D.; Kirk, K. L.; Poulsen, F. M.; Valeri, C. R.; Vecchione, J. J. *FEBS Lett.* **1981**, *136*, 325–328. (b) Diffley, D. M.; Costa, J. L.; Sokoloski, E. A.; Chiueh, C. C.; Kirk, K. L.; Creveling, C. R. *Biochem. Biophys. Res. Commun.* **1983**, *110*, 740–745.

(8) For recent examples of ^{19}F NMR probes for enzymatic analyses, see: (a) Mizukami, S.; Takikawa, R.; Sugihara, F.; Hori, Y.; Tochio, H.; Wälchli, M.; Shirakawa, M.; Kikuchi, K. *J. Am. Chem. Soc.* **2008**, *130*, 794–795. (b) Stockman, B. J. *J. Am. Chem. Soc.* **2008**, *130*, 5870–5871. (c) Tanabe, K.; Harada, H.; Narazaki, M.; Tanaka, K.; Inafuku, K.; Komatsu, H.; Ito, T.; Yamada, H.; Chujyo, Y.; Matsuda, T.; Hiraoka, M.; Nishimoto, S. *J. Am. Chem. Soc.* **2009**, *131*, 15982–15983. (d) Takaoka, Y.; Sakamoto, T.; Tsukiji, S.; Narazaki, M.; Matsuda, T.; Tochio, H.; Shirakawa, M.; Hamachi, I. *Nat. Chem.* **2009**, *1*, 557–561.

(9) (a) Cui, W.; Otten, P.; Li, Y.; Koeneman, K. S.; Yu, J.; Mason, R. P. *Magn. Reson. Med.* **2004**, *51*, 616–620. (b) Yu, J.; Mason, R. P. *J. Med. Chem.* **2006**, *49*, 1991–1999. (c) Liu, L.; Kodibagkar, V. D.; Yu, J.-X.; Mason, R. P. *FASEB J.* **2007**, *21*, 2014–2019. (d) Yu, J.-X.; Kodibagkar, V. D.; Liu, L.; Mason, R. P. *NMR Biomed.* **2008**, *21*, 704–712.

(10) Colibus, L. D.; Li, M.; Binda, C.; Lustig, A.; Edmondson, D. E.; Mattevi, A. *Proc. Natl. Acad. Sci. U.S.A.* **2005**, *102*, 12684–12689.

(11) Faint artifacts were observed in Figure 4b because of the excessive brightness of the samples.

(12) Arnett, C. D.; Fowler, J. S.; MacGregor, R. R.; Schlyer, D. J.; Wolf, A. P.; Lângstörn, B.; Halldin, C. *J. Neurochem.* **1987**, *2*, 522–527.